J Neurophysiol 95: 2222–2232, 2006.
First published December 7, 2005; doi:10.1152/jn.01014.2005.

Dissociated Hysteresis of Static Ocular Counterroll in Humans

A. Palla,[1] C. J. Bockisch,[1,2,3] O. Bergamin,[3] and D. Straumann[1]
[1]*Departments of Neurology,* [2]*Otorhinolaryngology, and* [3]*Ophthalmology, Zurich University Hospital, Zurich, Switzerland*

Submitted 27 September 2005; accepted in final form 4 December 2005

Palla, A., C. J. Bockisch, O. Bergamin, and D. Straumann. Dissociated hysteresis of static ocular counterroll in humans. *J Neurophysiol* 95: 2222–2232, 2006. First published December 7, 2005; doi:10.1152/jn.01014.2005. In stationary head roll positions, the eyes are cyclodivergent. We asked whether this phenomenon can be explained by a static hysteresis that differs between the eyes contra- (CE) and ipsilateral (IE) to head roll. Using a motorized turntable, healthy human subjects ($n = 8$) were continuously rotated about the earth-horizontal naso-occipital axis. Starting from the upright position, a total of three full rotations at a constant velocity (2°/s) were completed (acceleration = 0.05°/s^2, velocity plateau reached after 40 s). Subjects directed their gaze on a flashing laser dot straight ahead (switched on 20 ms every 2 s). Binocular three-dimensional eye movements were recorded with dual search coils that were modified (wires exiting inferiorly) to minimize torsional artifacts by the eyelids. A sinusoidal function with a first and second harmonic was fitted to torsional eye position as a function of torsional whole body position at constant turntable velocity. The amplitude and phase of the first harmonic differed significantly between the two eyes (paired *t*-test: $P < 0.05$): on average, counterroll amplitude of IE was larger [CE: 6.6 ± 1.6° (SD); IE: 8.1 ± 1.7°), whereas CE showed more position lag relative to the turntable (CE: 12.5 ± 10.7°; IE: 5.1 ± 8.7°). We conclude that cyclodivergence observed during static ocular counterroll is mainly a result of hysteresis that depends on whether eyes are contra- or ipsilateral to head roll. Static hysteresis also explains the phenomenon of residual torsion, i.e., an incomplete torsional return of the eyes when the first 360° whole body rotation was completed and subjects were back in upright position (extorsion of CE: 2.0 ± 0.10°; intorsion of IE: 1.4 ± 0.10°). A computer model that includes asymmetric backlash for each eye can explain dissociated torsional hysteresis during quasi-static binocular counterroll. We hypothesize that ocular torsional hysteresis is introduced at the level of the otolith pathways because the direction-dependent torsional position lag of the eyes is related to the head roll position and not the eye position.

INTRODUCTION

Compensatory steady-state eye positions, evoked by reorienting the head with respect to gravity and keeping the head still, are static (velocity ≈ 0°/s). When the head is tilted about the naso-occipital axis, the head movement is called head roll and the compensatory eye movements ocular counterroll (Nagel 1868). The vestibular signal that drives ocular counterroll in static head roll positions or during very slow, i.e., quasi-static, head roll displacements, is exclusively otolithic (Diamond et al. 1979; Seidman et al. 1995) and predominantly originates from the utricles (Diamond and Markham 1983; Markham et al. 1973; Suzuki et al. 1969). Static (or quasi-static) ocular counterroll (SOCR) compensates for only ~5–25% of head roll, with the highest values around upright head position (Averbuch-Heller et al. 1997; Collewijn et al. 1985; Kingma et al. 1997; Krejcova et al. 1971; Ott et al. 1992; Pansell et al. 2003; Schworm et al. 2002). Vision is not hampered by the limitation of SOCR, because stereo acuity is relatively tolerant to fluctuations of binocular disparity (Van Rijn et al. 1994). It has been suggested that SOCR represents a remnant from lateral-eyed animals or reflects a motor control strategy related to spatial orientation (Angelaki and Hess 1996a,b).

SOCR is sustained during fixations, saccades, and smooth pursuit eye movements (Haslwanter et al. 1992; Hess and Angelaki 2003). It is likely that the tonic signal for SOCR is provided by the neural torsional velocity-to-position integrator (Crawford et al. 2003; Glasauer et al. 2001), whereas the contributions of extravestibular signals, such as neck proprioception (Ott et al. 1992) and vision (Diamond et al. 1979), are small or absent. Recently, a decrease of SOCR during sustained head tilt has been described (Pansell et al. 2005; Seidman et al. 1995; Yashiro et al. 1996). Whether this drift reflects a deficiency in the neural torsional velocity-to-position integrator (Seidman et al. 1995) or visual adaptation to spatial verticality (Yashiro et al. 1996) is unclear.

Since the pioneering studies on SOCR in healthy human subjects by Diamond and colleagues (Diamond and Markham 1983; Diamond et al. 1979) and Collewijn et al. (1985), investigators have been hesitant in interpreting recorded torsional disconjugacies between the two eyes. Diamond and Markham observed the following pattern of SOCR during quasi-static 360° whole body roll movements (velocity: 3°/s; acceleration 0.21°/s^2) (Diamond et al. 1979): *1*) ocular counterroll was not always conjugate, i.e., torsional differences around 2° between the two eyes were not uncommon in individual subjects; *2*) there was more counterrolling of the lowermost than of the uppermost eye; and *3*) some subjects showed consistent differences of ocular counterroll at specific whole body orientations, which depended on whether this orientation was reached by a right ear-down or left ear-down rotation. In another study, the same authors found similar disconjugacies of torsional eye position ≤4°, when subjects were kept for 10 min in different whole body ear-down positions ≤90° from upright (Diamond et al. 1982). Although possible physiological mechanisms were considered by the authors, the measured torsional disconjugacy was attributed mainly to imprecision of three-dimensional eye movement measurements. Collewijn et al. (1985), who were the first to perform experiments on SOCR using dual search coils, also came to the conclusion that binocular torsion in static head roll positions was basically conjugate.

Address for reprint requests and other correspondence: A. Palla, Neurology Dept, Zurich Univ. Hospital, Frauenklinikstrasse 26, CH-8091 Zurich, Switzerland (E-mail: antpalla@access.unizh.ch).

The costs of publication of this article were defrayed in part by the payment of page charges. The article must therefore be hereby marked "*advertisement*" in accordance with 18 U.S.C. Section 1734 solely to indicate this fact.

Closer analysis of binocular SOCR increasingly cast its conjugacy into doubt. In a monocular dual search-coil study, Bockisch and Haslwanter (2001) recently observed a specific pattern of SOCR asymmetry, in which consistently less ocular torsion was noted when subjects were rolled toward the side of the measured eye. This finding was ascribed to a mechanical inhibition of search coil annulus intorsion by the nasally exiting lead wire touching the lower lid. Using binocular video-oculography, however, Pansell et al. (2003) and Schworm et al. (2002) confirmed the observation that the intorting eye shows less counterroll than the extorting eye at static head roll positions $\leq 45°$ from upright. The same authors, in addition, reported another interesting finding on SOCR: after head reorientation from the 45° static head roll position, the eyes did not completely rotate back to the initial torsional position measured before the head tilt, but settled at a torsional offset position in the direction of the previous counterroll (Schworm et al. 2002). Taken together, the available data on binocular counterroll are inconsistent and do not yet allow conclusions on the significance and possible mechanisms of cyclovergence during and incomplete reversal after ocular counterroll. In particular, technical inaccuracies, different amplitudes of static head roll, and ongoing influences of dynamic ocular responses evoked by rapid displacements between static head positions might have influenced the outcome of the cited investigations.

The purpose of our study was to carefully re-examine binocular counterroll during static head roll. By using modified dual search coils with wires exiting inferiorly, we reduced torsional artifacts by the eyelids (Bergamin et al. 2002). Whole body rotations on a motorized turntable avoided eye position changes induced by the cervico-ocular reflex. Dynamic influences on static counterroll were excluded by recording eye movements during very slow, i.e., quasi-static, continuous turntable rotations. Finally, completing three full turntable rotations allowed us to characterize the critical parameters of initial and steady-state behavior of SOCR during whole body roll.

Portions of this work were presented previously in a conference proceeding (Palla et al. 2005).

METHODS

Definitions

We term ocular counterroll during constant-velocity whole body rotation about the earth-horizontal naso-occipital axis as "quasi-static" if the velocity is low (2°/s) and the initial acceleration to reach the velocity plateau is below the detection threshold of the semicircular canals ($0.05°/s^2$). The direction of turntable rotation is defined from the subject's viewpoint: clockwise corresponds to a rotation beginning with right ear moving down.

Subjects

Eight healthy human subjects (4 female; 30–42 yr old) participated in this study. Informed consent of all subjects was obtained after full explanation of the experimental procedure. The protocol was approved by a local ethics committee and was in accordance with the ethical standards from the 1964 Declaration of Helsinki for research involving human subjects.

Experimental setup

Subjects were seated upright on a turntable with three servo-controlled motor driven axes (prototype built by Acutronic, Jona, Switzerland). The head was restrained with an individually molded thermoplastic mask (Sinmed, Reeuwijk, The Netherlands). Subjects were positioned so that the intersection of the interaural and naso-occipital axes was at the intersection of the three axes of the turntable. Pillows and safety belts minimized movements of the body. A turntable-fixed aluminum coil frame (side length 0.5 m) surrounded the head and generated three orthogonal digitally synchronized magnetic wave fields of 80, 96, and 120 kHz. A digital signal processor computed a fast Fourier transform in real-time on the digitized search coil signal to determine the voltage induced on the coil by each magnetic field (system by Primelec, Regensdorf, Switzerland). Coil orientation could be determined with an error of $<7\%$ over a range of $\pm 30°$ and with a noise level of $<0.05°$ (root mean squared deviation).

Recording of eye and turntable rotation

Three-dimensional (3D) eye movements were recorded binocularly with dual scleral search coils (Skalar Instruments, Delft, The Netherlands). In this study, we only report on torsional eye movements. To minimize torsional artifacts by mechanical interaction of the nasally exiting wire of the search coils with the upper and lower eyelids, modified search coils with the wire exiting inferiorly (~6 o'clock) were used. Coil modifications were performed with the technique described by Bergamin et al. (2002).

Because the coil frame was firmly fixed to the turntable, we had to derive the position of the head in space from the position signal of the earth-horizontal axis about which the turntable rotated. To confirm that the head was fixed to the turntable during full whole body rotations about the naso-occipital axis, we attached a head coil on the forehead in two subjects. The peak-to-peak torsional displacement of the head in the coil frame did not exceed 0.5°. Eye and turntable position signals were digitized at 1,000 Hz per channel with 12-bit resolution and stored on a computer hard disk for off-line processing.

Experimental protocol

Starting from the upright position, subjects were rotated about their earth-horizontal naso-occipital axis clockwise (CW) or counterclockwise (CCW) at a constant angular velocity of 2°/s. To reach this velocity plateau, the turntable was accelerated by $0.05°/s^2$, which is below the detection threshold of the semicircular canals (Diamond et al. 1982; Shimazu and Precht 1965). The acceleration phase lasted 40 s. A total of three consecutive 360° turntable rotations were performed before the turntable was stopped. To exclude ocular torsion related to gaze direction, e.g., when Listing's plane is not exactly aligned with the frontal plane of the coordinate system, a space-fixed laser dot was projected along the axis of rotation onto a spherical screen at a distance of 1.4 m. Every 2 s, the laser dot was turned on for a duration of 20 ms. Subjects were instructed to look at the laser dot and to keep their eyes at this position during the off periods. The short-duration of on periods ensured that the smooth pursuit system was not activated. Experiments were performed in otherwise total darkness.

To determine a possible dynamic contribution to quasi-static ocular counterroll, seven subjects were additionally rotated at constant velocities of 1, 4, and 8°/s in the CW direction. The initial turntable acceleration was unchanged, i.e., $0.05°/s^2$. The velocity plateaus were reached after 20, 80, and 160 s, respectively. Thus two consecutive 360° turntable rotations at constant velocity were performed before the turntable was stopped. Two subjects were also rotated stepwise between static whole body roll positions. The steps consisted of velocity triangles with a peak acceleration of 10 or $0.05°/s^2$. The step

amplitude was 90°, and each position at 0, 90, 180, 270, and 360° was held for 60 s.

Data analysis

Search coil signals from both eyes were processed with interactive programs written in MATLAB (MathWorks, Natick, MA). 3D eye positions were computed as rotation vectors (Haustein 1989). The sign of the torsional component of a rotation vector is determined by the right-hand rule, i.e., CW torsion, as seen by the subject, is positive. For convenience, torsional eye position was converted to degrees.

For reference, torsional eye positions of both eyes immediately before the beginning of the turntable rotation were set to zero. This was achieved by averaging over an interval of 3–5 s before turntable rotation and subtracting this value from the whole torsional position trace. Eye position data during blinks were interactively selected and removed.

Torsional eye position was analyzed as a function of torsional turntable position. For each turntable rotation cycle, the following sine function with two harmonics was fitted to the data

$$y = A \times \sin(\omega t + \varphi_1) + B \times \sin(2 \times \omega t + \varphi_2) + c$$

where A is the amplitude of the first harmonic and B the amplitude of the second harmonic, ω the frequency, φ_1 and φ_2 are the phases of the first and second harmonic, respectively, and C the offset. Note that the second harmonic describes the periodic deviation from an ideal sinusoidal function and is, by definition, twice the frequency of the first harmonic.

RESULTS

Figure 1 shows torsional eye position of both eyes plotted against torsional turntable position in a typical subject (A.P.). Starting from the upright position, three complete rotations about the earth-horizontal naso-occipital axis were performed in CCW and CW directions. During turntable rotations, the eyes did not always move conjugately but started to diverge around the middle of the first hemicycle of whole body roll, i.e., the 90° ear-down position. Cyclodivergence reached a maximum around the 180° whole body position. This pattern of maximal cyclodivergence in upside-down position was observed for both CCW (Fig. 1, *top*) and CW (Fig. 1, *bottom*) turntable rotations and was apparent during all three roll cycles.

Figure 2 depicts torsional eye positions in consecutive upright and upside-down positions of the same subject as in the previous figure (circles: right eye torsional positions; squares: left eye torsional positions). To avoid possible contamination by blinks or saccades, average torsion of both eyes was computed over intervals of turntable positions ±10° around upright and upside-down whole body positions, respectively. Recall that, for reference, ocular torsion at the initial upright turntable position was defined as zero (see METHODS).

The example in Fig. 2 shows typical features seen in all subjects. *1*) After the first rotation cycle, both eyes did not completely return to zero torsion. For CCW, the right eye was still in an intorsional position and the left eye in an extorsional position. Likewise, for CW rotation, the right eye was extorted, whereas the left eye was intorted. This residual torsion (RT), i.e., the remaining amount of torsional eye position appearing after the first roll cycle, was effectively unchanged after the second and third rotation cycles in either direction. *2*) During both CCW and CW whole body rotations, the eye contralateral to head roll (CE) always lagged the turntable when it arrived in the upside-down position, whereas the other eye, i.e., the eye ipsilateral to head roll (IE), showed some asymmetry between CCW and CW rotation, but was always closer to zero than CE. Thus independent of the rotation direction, the eyes cyclodiverged during the first hemicycle of rotation and cyclocon-

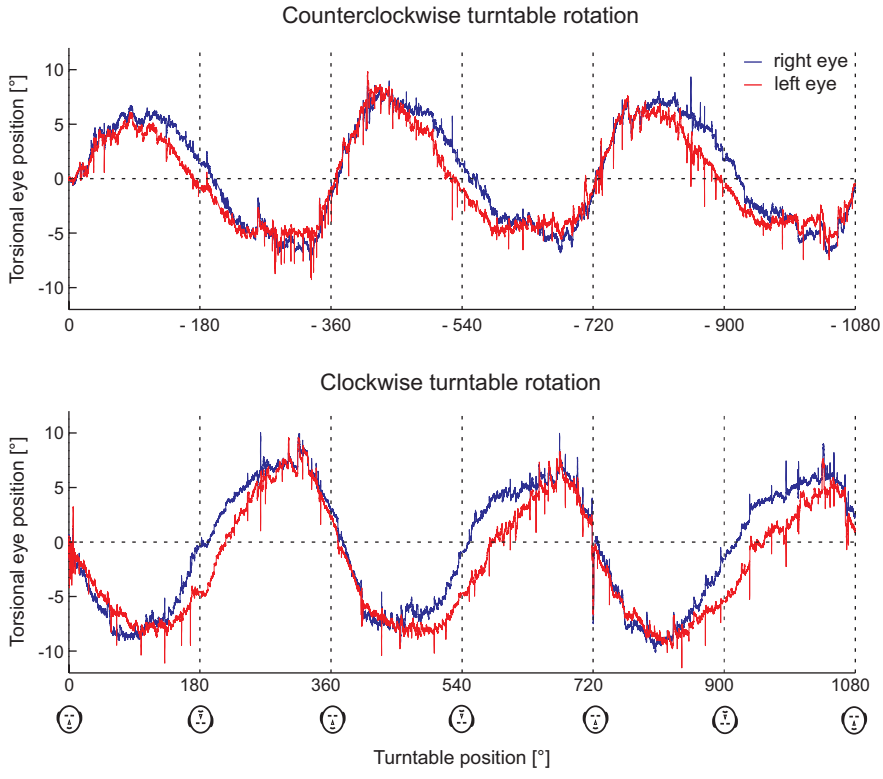

FIG. 1. Example of binocular torsional position plotted as a function of whole body roll position in a subject (A.P.). Starting from the upright position, 3 full turntable rotations were applied. *Top*: counterclockwise (CCW) turntable rotation. *Bottom*: clockwise (CW) turntable rotation. Blue traces, right eye; red traces, left eye. CW eye torsion, as seen by the subject, is positive. For reference, torsional eye position of both eyes at the initial upright whole body position was set to 0.

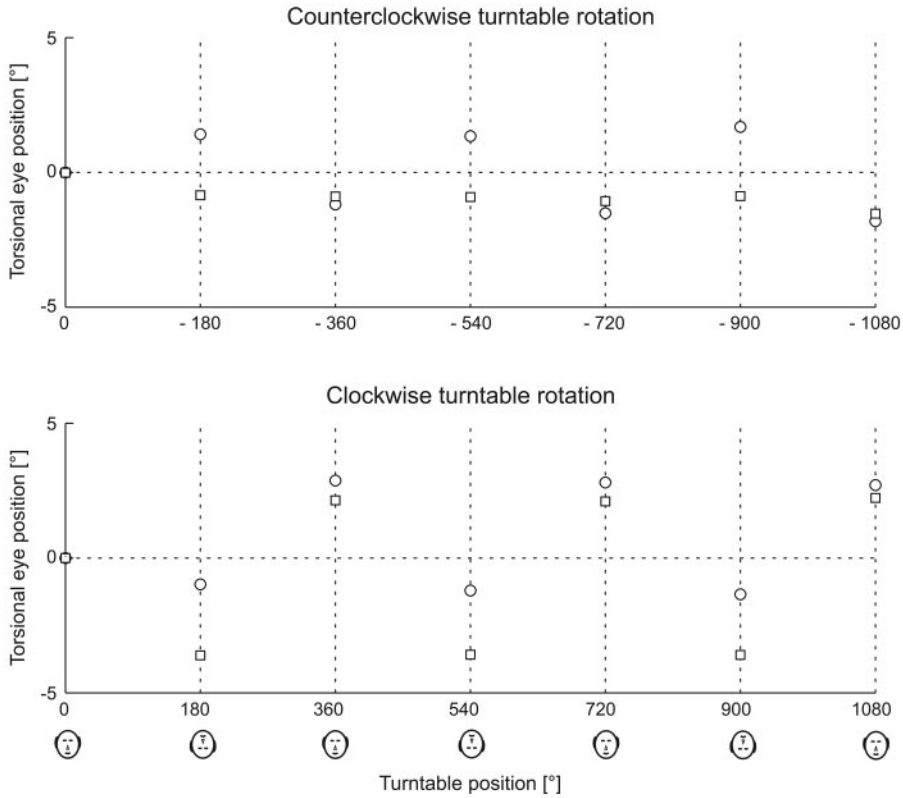

FIG. 2. Example of average torsional eye positions (same subject as in Fig. 1) determined for intervals of turntable positions ±10° around whole body upright (±360, ±720, and ±1,080°) or upside-down (±180, ±540, and ±900°) positions. *Top*: CCW turntable rotation. *Bottom*: CW turntable rotation. Circles, right eye; squares, left eye. Reference 0 torsion and definition of direction as in Fig. 1.

verged during the second hemicycle. Note that, in this particular example, the torsional position of the left eye during CCW rotation (Fig. 2, *top*) was similar in upright and upside-down positions, but not during CW rotation; the pattern of more cyclodivergence in upside-down positions, however, was about the same for CCW and CW rotations.

Figure 3 summarizes the findings on RT in all eight subjects tested. Average positions of both eyes (circle, right eye; square, left eye) in upright position are depicted after the first, second, and third full rotation. RT always emerged after the first full rotation and did not significantly change with the two subsequent rotations, i.e., torsion after the first, second, and third rotation was not significantly different (ANOVA: $P > 0.05$). Average RT was significantly (*t*-test: $P < 0.05$) larger in CE (left eye after 1st CW rotation: 2.2 ± 0.10°; right eye after 1st CCW rotation: −1.8 ± 0.13°) than in IE (right eye after 1st CW rotation: 1.7 ± 0.10°; left eye position after 1st CCW rotation: −1.0 ± 0.10°).

To analyze the steady-state behavior of binocular counterroll, we focused on the two full rotation cycles during constant turntable velocity, i.e., the second and third cycle. For the same example as in Figs. 1 and 2, Fig. 4 depicts binocular torsion during the second full roll cycle. The *left column* corresponds to the data recorded during rotation in the CW direction; the *right column* corresponds to the data recorded during rotation in the CCW direction. Note that CW rotation starts from 0° in the positive direction (arrow to the *right*) and CCW from 360° in the negative direction (arrow to the *left*).

Torsional eye position traces of both eyes as a function of turntable roll position (Fig. 4, *A* and *B*) were fitted with

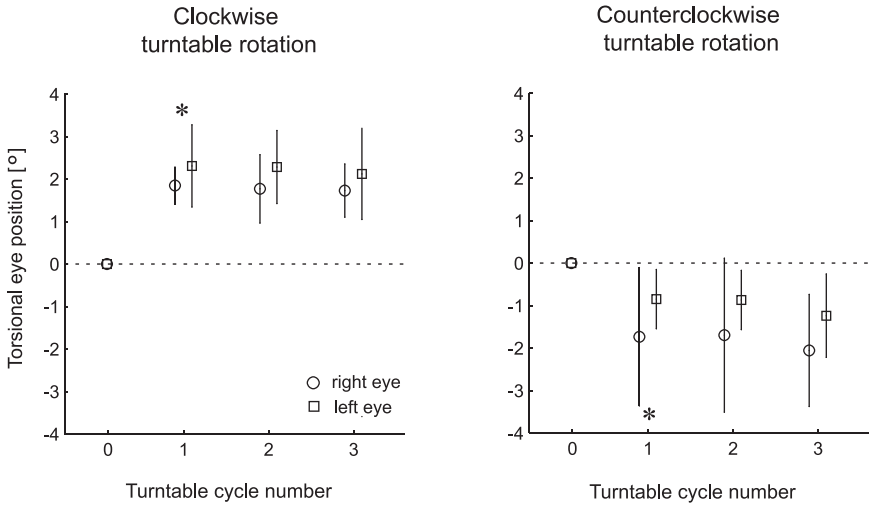

FIG. 3. Residual torsion in upright position after the 1st, 2nd, and 3rd whole body rotation. Average of all 8 subjects tested (error bars: ±SD). Torsion before the 1st rotation is referenced to 0. *Left*: CW turntable rotation. *Right*: CCW turntable rotation. Circles, average of right torsional eye positions; squares, average of left torsional eye positions. Note that residual torsion after the 1st rotation was significantly different between the 2 eyes both in the CCW and CW roll direction (*$P < 0.05$ in paired *t*-test).

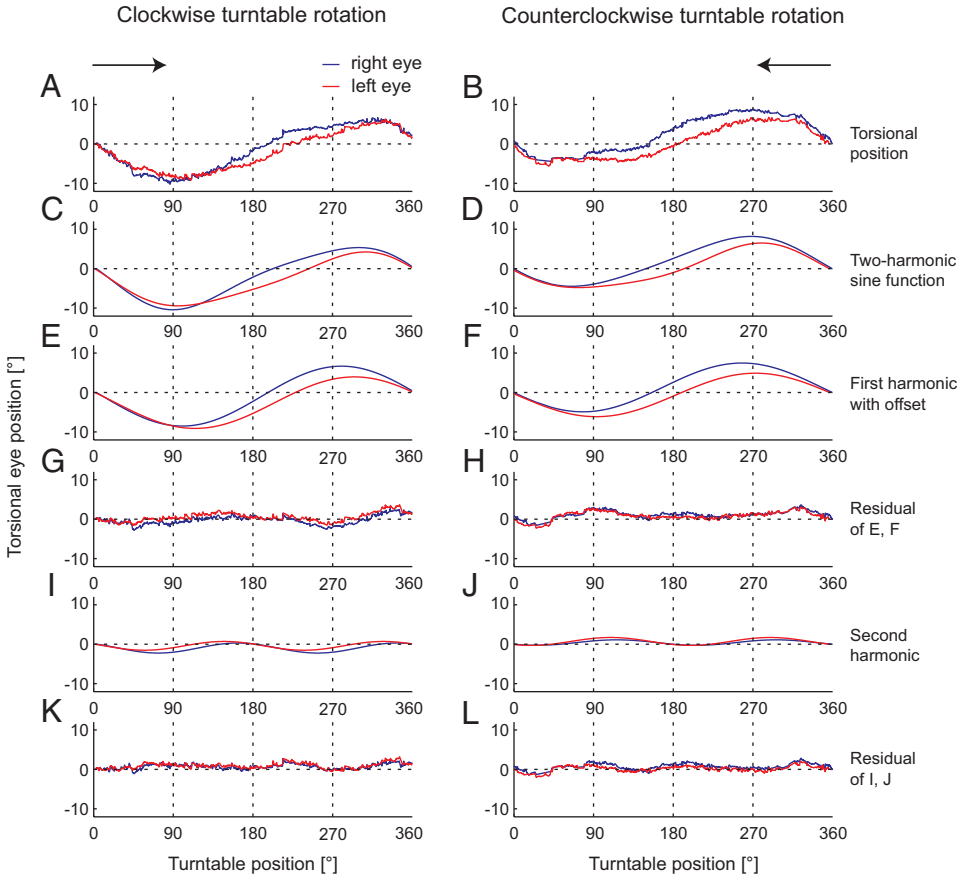

FIG. 4. Example of binocular torsion during the 2nd roll cycle and subsequent mathematical analysis (same subject as Figs. 1 and 2). *Left*: data derived from turntable rotation in the CW direction (arrow to the *right*: rotation started from 0° in positive direction). *Right*: data derived from turntable rotation in the CCW direction (arrow to the *left*: rotation started from 360° in negative direction). CW eye torsion, as seen by the subject, is positive. Blue traces, right eye; red traces, left eye. *A* and *B*: torsional eye position of both eyes plotted as a function of turntable position. *C* and *D*: 2-harmonic sine function fitted to torsional eye position as a function of turntable position. *E* and *F*: 1st harmonic of the fitted 2-harmonic sine function with offset. *G* and *H*: residual data after subtraction of the 1st harmonic and offset. *I* and *J*: 2nd harmonic of the fitted 2-harmonic sine function. *K* and *L*: residual data after subtraction of the full 2-harmonic sine function. Note that the 1st harmonic together with the offset (*E* and *F*) already contains a major fraction of the data.

sinusoidal functions composed of a first and a second harmonic (Fig. 4, *C* and *D*; see METHODS). The first harmonic together with the offset (Fig. 4, *E* and *F*) already comprised a major fraction of the data, i.e., the residual data (Fig. 4, *G* and *H*) was confined to a narrow range (<3°) around zero torsion. As a result, the amplitude of the second harmonic (Fig. 4, *I* and *J*) was considerably smaller than the amplitude of the first harmonic. Accordingly, the further decrease of residual data (Fig. 4, *K* and *L*) was unimpressive. Introducing a third harmonic did not significantly ($P > 0.05$) decrease residual torsional eye position in any subject (data not shown).

Analyzing the first harmonic (Fig. 4, *E* and *F*) explains the main features of binocular counterroll in both directions. In the following, the terms "amplitude" and "phase" apply to the first harmonic of the two-harmonic sine fit. Before fitting, the torsional eye trajectories were shifted along the ordinate such that zero torsion was in upright whole body position. During CW roll (Fig. 4*E*), amplitudes of the two eyes were similar (right eye: 8°; left eye: 7°); phases, however, differed by 15° (right eye: −10°; left eye: −25°) with CE (left eye) lagging more than IE (right eye). During CCW roll (Fig. 4*F*), the behavior of the two eyes was similar. Again, amplitudes were almost equal (both eyes: 6°) and phases differed by 15° (right eye: 12°; left eye: −3°), with CE (right eye) lagging more than IE (left eye). In fact, for this roll direction, IE slightly lead the turntable. Note that, in this plot, a position lag is indicated by a negative phase in the CW direction and a positive phase in the CCW direction.

Figure 5 summarizes the amplitude and phase of the first harmonic of the two-harmonic sine fit (including an offset) in all eight tested subjects. The fit values were obtained from the second or third roll cycle. The criterion for choosing the cycle was based on fewer blinks. Right and left eyes were pooled from CW and CCW rotations.

The average amplitude differed significantly (paired *t*-test: $P < 0.01$) between CE and IE (Fig. 5, *left*), i.e., the average amplitude of CE was 17% smaller (CE: 6.6 ± 1.6°; IE: 8.1 ± 1.7°). CE showed a significantly (paired *t*-test: $P < 0.01$) larger

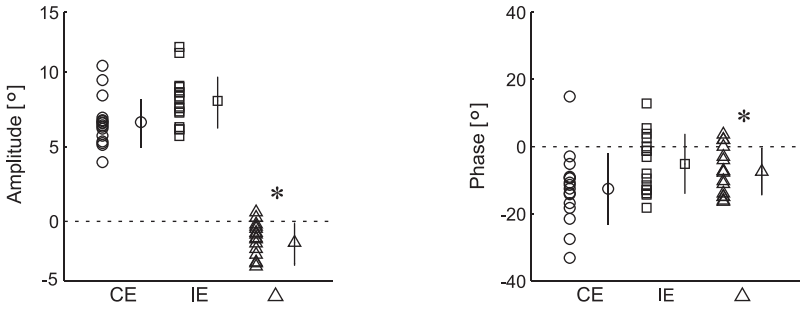

FIG. 5. Amplitudes and phases of the 1st harmonic of the 2-harmonic sine fit in all 8 subjects. Circles, pooled eyes contralateral to head roll (CE); squares, pooled eyes ipsilateral to head roll (IE). CE corresponds to left eyes for CW and right eyes for CCW rotations. Conversely, IE corresponds to right eyes for CW and left eyes for CCW rotations. Triangles, interindividual differences (Δ) between CE and IE. On the *right* of each population of data points, average values ± SD (symbols with error bars) are plotted. Note the significant differences between CE and IE in amplitude and phase (*$P < 0.01$ in paired *t*-test). Recall that phase lag represents position lag because torsional eye position is analyzed as a function of turntable position.

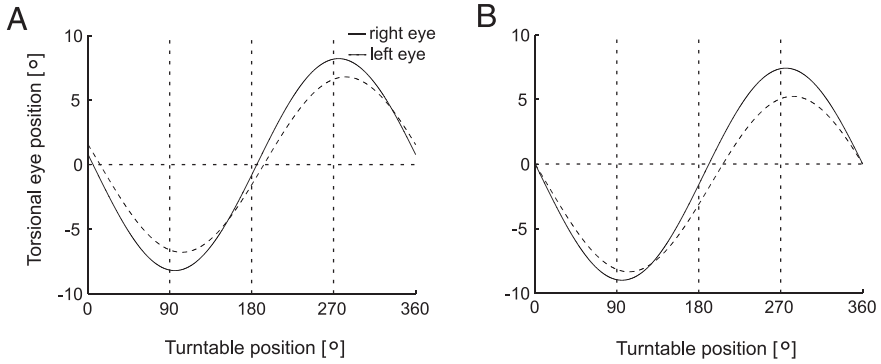

FIG. 6. Two-harmonic sine fits of averaged binocular eye torsion over all subjects during steady-state CW rotation. Continuous lines, fit of eyes ipsilateral to head roll (right eye); dashed lines, fit of eyes contralateral to head roll (left eye). *Left*: offset coincides with 0 baseline. *Right*: curves referenced to 0 in upright whole body position.

position lag than IE, as computed from the phase values of the first harmonic (Fig. 5, *right*). The difference of average position lags between the two eyes was 7.4° (CE: −12.5 ± 10.7°; IE: −5.1 ± 8.7°). Amplitude and phase of the second harmonic were not significantly different between CE and IE (paired *t*-test: $P > 0.05$; data not shown).

Figure 6 shows fitted average binocular torsion of all subjects during CW roll. For the *left panel* (Fig. 6*A*), the offset of the fit is set to zero, i.e., maximal absolute torsion above and below the zero baseline is equal. For the *right panel* (Fig. 6*B*), however, torsion was set to zero in the upright whole body position.

The shifting of curves to zero at upright whole body position for reference (Fig. 6*B*) has several consequences: *1*) binocular torsion becomes relatively conjugate during the first 90–120° of roll, before the eyes increasingly cyclodiverge; *2*) the absolute values of maximal intorsion and extorsion become different, whereby the difference is larger for CE (as it lags the turntable more than IE); *3*) maximal absolute torsion becomes larger during the first and smaller during the second hemicycle; and *4*) cyclodivergence measured in the upside-down position increases further.

Figure 7 compares values derived from the two-harmonic sine fits between CE and IE. The maximal absolute torsional positions for CE and IE during CW and CCW roll are compared in the *top panels* (Fig. 7, *A* and *B*): on average, maximal extorsion, reached by an eye during the first rotation hemicycle, amounted to 7.9 ± 2.4°, whereas maximal extorsion reached during the second rotation hemicycle was 7.1 ± 2.0° (Fig. 7*A*). This difference was significant (paired *t*-test: $P < 0.01$). Average maximal intorsion during the first rotation hemicycle was 9.3 ± 2.0° and during the second rotation hemicycle was 5.4 ± 1.7° (Fig. 7*B*). Again, this difference was significant (paired *t*-test: $P < 0.01$). Consequently, whether the eye extorted during the first, i.e., corresponding to CE, or second hemicycle, i.e., corresponding to IE, resulted in different amounts of maximal torsional eye positions. The same was true for intorsion during the first or second hemicycle. Eye torsion in the upside-down position also depended on the roll direction (Fig. 7*C*). On average, CE was extorted by 2.9 ± 2.4° and IE was intorted by 1.4 ± 2.3° (paired *t*-test: $P < 0.01$). Thus in the upside-down position, the torsional orientation of an eye was different depending on whether the upside-down position had been reached by a CW or CCW rotation. As a

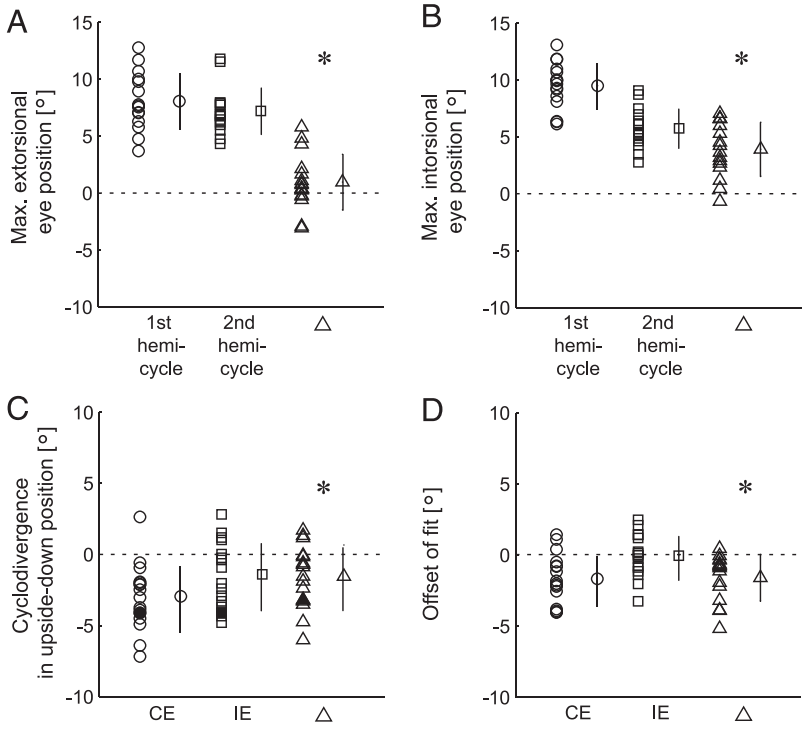

FIG. 7. Comparison of maximal torsional eye positions, cyclodivergences, and torsional eye position offsets in all 8 subjects. Data pooling and symbols as in Fig. 5. *A*: maximal extorsional eye position. *B*: maximal intorsional eye position. *C*: cyclodivergence in upside-down position. *D*: offset of fitted 2-harmonic sine fit. *$P < 0.01$ in paired *t*-test.

result, the average offsets of the fitted two-harmonic sinusoidal functions differed significantly ($P < 0.01$) between the extorting ($-1.7 \pm 1.7°$) and intorting ($-0.08 \pm 1.5°$) eyes (Fig. 7*D*).

We asked whether the results for whole body roll are representative for SCOR. If this were the case, increasing or decreasing the velocity by a few degrees per second should not change counterroll behavior. In seven of the eight subjects tested previously, we therefore compared steady-state ocular counterroll of the right eye among trials with velocities of 1, 2, 4, and 8°/s in the CW direction. The statistical comparison of the two-harmonic sine fits (amplitudes, phases, offset) among the four velocities yielded no significant differences (1-way ANOVA: $P > 0.05$).

In two subjects we compared ocular counterroll during quasi-static turntable rotation, i.e., low constant velocity whole body roll, with ocular counterroll during "true" static conditions, i.e., stepwise fast (peak acceleration: 10°/s^2) or slow (peak acceleration: 0.05°/s^2) turntable rotations to consecutive static whole body roll positions. Figure 8 shows the data in one subject (D.S.); the data in the other subject (A.P.) was qualitatively similar. Both stepwise static roll (fast: Fig. 8*A*; slow: Fig. 8*B*) and continuous roll (Fig. 8*C*) in the CW direction led to cyclodivergence in the upside-down position, with IE (right eye) intorsion close to zero, but CE (left eye) extorsion around 5°. During the second hemicycle of continuous whole body roll (Fig. 8*C*), cyclodivergence decreased and torsion of both eyes approached zero baseline. In contrast, cyclodivergence during the stepwise static paradigms (Fig. 8, *A* and *B*) did not become smaller during the 90° roll steps from upside-down back to upright. In this subject and similarly in the other subject tested (data not shown), stepwise turntable rotations evoked various amounts of cyclovergence, which became, with each roll step from the reference upright position, increasingly different from the quasi-static data. The "true" static, i.e., stepwise, paradigms (Fig. 8, *A* and *B*) differed in that the amount of cyclodivergence in upside-down position and in the final upright position was smaller, when the steps were slow (Fig. 8*B*). This finding could be attributed to the absence of occasional saccade-like, anticompensatory eye movements (Fig. 8*A*, arrows) associated with the roll steps at higher acceleration (Schworm et al. 2002). Strikingly,

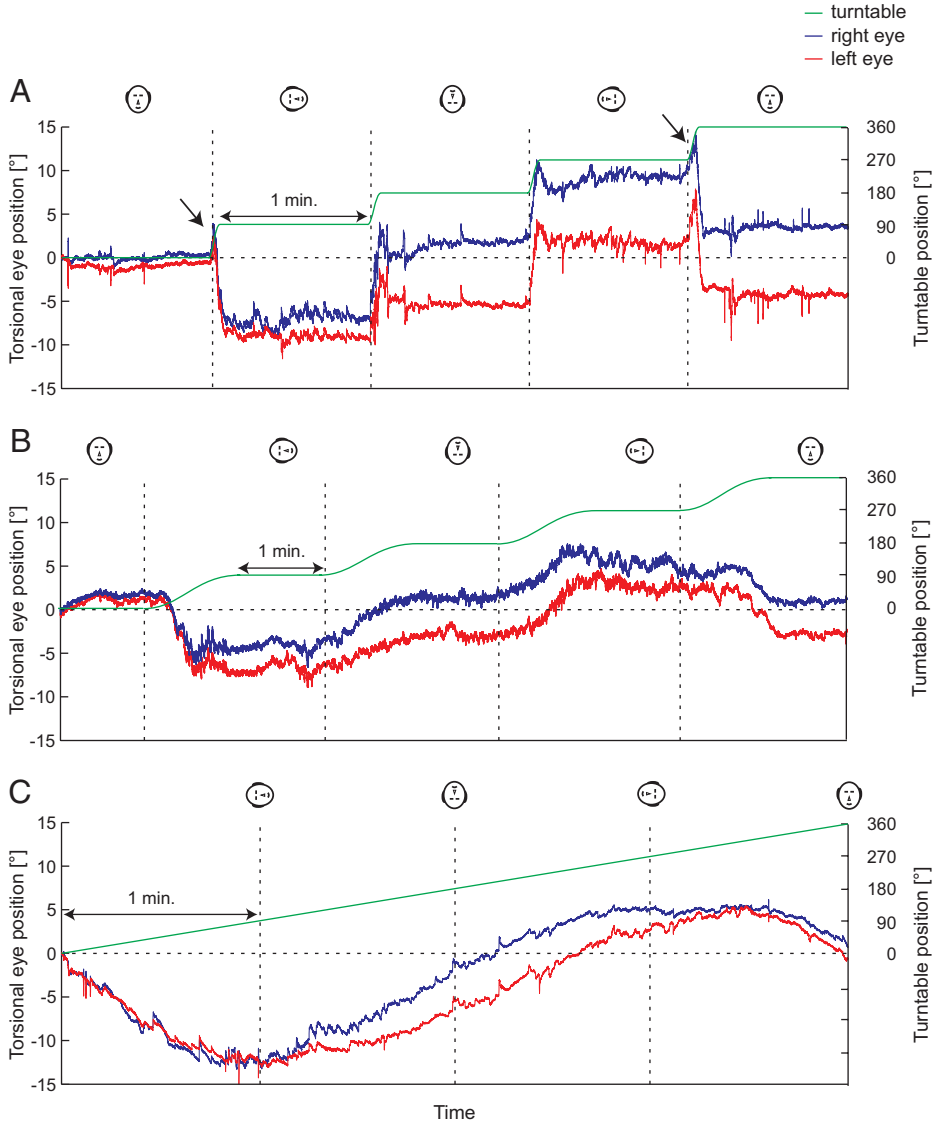

FIG. 8. Example of binocular torsional position plotted as a function of time in a subject (D.S.). *A*: stepwise CW whole body roll to 0, 90, 180, 270, and 360° turntable positions with peak acceleration of 10°/s^2. *B*: stepwise CW whole body roll to 0, 90, 180, 270, and 360° turntable positions with peak acceleration of 0.05°/s^2. *C*: 360° constant velocity CW whole body roll. Blue traces, right eye; red traces, left eye; green traces, turntable position. For reference, torsional eye position of both eyes at initial upright position was set to 0. Arrows, occasional saccade-like, anticompensatory eye movements at the beginning of roll steps. Note different time scales in subplots. Ordinate scale for turntable position is indicated on *right* of subplots.

ocular torsion during stepwise roll, even when performed with very low acceleration, fluctuated substantially more than during the quasi-static paradigm.

DISCUSSION

We analyzed the static binocular counterroll of healthy human subjects during constant low-velocity whole body rotations about the naso-occipital axis. After the first full rotation from the initial upright position, both eyes displayed a torsional offset in the direction of the previous counterroll. This residual torsion was consistently larger in the eye contralateral to head roll (CE) than in the eye ipsilateral to head roll (IE), and was unchanged after consecutive rotation cycles. When rolling toward the upside-down position the eyes cyclodiverged. In the upside-down position, the amount of CE extorsion was always larger than the amount of IE intorsion. This cyclodivergence decreased when subjects were rolled further back to the upright position. In the following, we provide a rationale of the experimental setup and parameters and compare our results on static binocular counterroll with previous work by others.

Rationale of experimental setup and parameters

Strictly speaking, the applied torsional vestibular stimulus was "dynamic" in the sense that the turntable was always moving, but considering its low constant velocity, we regard the stimulus as quasi-static. Choosing a turntable velocity below 1°/s, to make the stimulus "more static", would have increased the duration of the period during which the subject's head is situated below the center of the body to unacceptable lengths. By repeating parts of the experiments with various velocity plateaus, we were able to show that, within the velocity range of 1–8°/s, turntable velocity does not influence the analyzed parameters.

Typically, SOCR is elicited by tilting the head sideways to a particular position, where it is held steady. Because a displacement between two static roll positions is dynamic by nature and, in addition, may evoke anticompensatory saccade-like movements (Schworm et al. 2002), we cannot be sure whether the subsequent steady-state torsional position of the eye is influenced by the previous dynamic ocular motor response. Another disadvantage of stepwise changes is that the drift from the initial torsional eye position after the roll displacement to the steady-state torsional eye position can last up to several minutes (Pansell et al. 2003). The strain on subjects from waiting for the end of the ocular drift would be unacceptable in upside-down positions.

In two subjects, we compared the quasi-static paradigm with ocular counterroll elicited by stepwise whole body roll displacements in 90° steps. In accordance to experiments by Markham and Diamond (2001), the stepwise paradigms tended to produce larger variations in eye torsion and cyclovergence than continuous roll, even at a very low acceleration of 0.05°/s^2. Because eye torsion became increasingly different from the quasi-static data with the growing number of roll steps, we cannot rule out that at least part of this variation was caused by torsional slippage of the coil during the fast torsional movements evoked by roll displacements. The fact, however, that the irregularity of ocular torsion during stepwise whole body roll was also present at in the slow acceleration paradigm supports the hypothesis that the otolithic membrane moves in patches, as suggested by Markham and Diamond (2001). Despite such variations, the fact that cyclodivergence of the eyes in the upside-down position was visible during both stepwise and continuous whole body roll underlines the robust nature of this finding.

Cyclovergence during SOCR

We showed that, during whole body rotations in the roll plane, the torsional positions of the two eyes are, in general, disconjugate. We explain this phenomenon of cyclodivergence by the existence of static hysteresis. The term "hysteresis" describes a property of systems whose states depend on their immediate history. More specifically, hysteresis is a lagging or retardation of the effect, when the forces acting on a body are changed (Webster definition). Hysteresis is considered to be static if it depends solely on position, i.e., not on time-critical factors such as velocity. Referring to our results, static hysteresis accounts for the finding that OCR at a given whole body position is not unequivocally determined by this whole body position, but depends on the previous history of whole body position. In other words, for a specific whole body position, OCR is determined by the direction from which the whole body position was reached.

The first fundamental study on binocular counterroll used a similar paradigm as in this study (Diamond et al. 1979): subjects were rotated with a constant velocity of 3°/s around the naso-occipital axis. Torsional eye position was measured from photographs taken of the whole upper part of the face. Similar to our results, the authors observed torsional disconjugacies $\leq 2°$. Interestingly, in contrast to our study, the authors reported of more counterroll in IE than in CE and of more binocular counterrolling during the hemicycle with the right ear-down, independent of whether this occurred during the first (right ear-down rotation) or second (left ear-down rotation) hemicycle. To explain these results, the authors postulated an asymmetry on the level of the otolith organs. As we will show below by simulating our data with a computer model, this observation could be the results of a bias, i.e., a baseline shift caused by torsional hysteresis, which was not taken into account when defining zero torsion for reference.

Direction-asymmetric hysteresis

The torsional position of either eye at a given turntable position was different depending on whether this turntable position was reached by a rotation in the CCW or CW direction. For example, at the 180° turntable position, the right eye was more extorted when it was the eye contralateral to head roll during the first hemicycle (CCW turntable rotation) than intorted when it was the eye ipsilateral to head roll (CW turntable rotation). This finding of different amounts of torsional hysteresis depending on whether the eyes are ipsi- or contralateral to head or whole body roll indicates that static torsional hysteresis is directionally asymmetric, i.e., dissociated.

Markham and Diamond were the first to use the term hysteresis to describe direction specific-properties of SOCR (Diamond et al. 1979). They drew the conclusion, however, that the observed hysteresis was not linked to the direction of

whole body roll but to the sequence of CW and CCW trials in their experiments.

Residual torsion

A major finding of this study is that, after the first 360° roll rotation, the torsional positions of both eyes differed from the torsional eye positions determined before the start of the rotation. We call this phenomenon residual torsion (RT) (Palla et al. 2005).

Recently, a similar observation was made by Schworm et al. (2002) for a different head roll paradigm with subjects laterally flexing their neck: ocular torsion evoked in consecutive head roll positions of 0, 15, 30, and 45° to the right or left was measured with 3D video-oculography. Each head position was held for 10 s. After the final head reorientation from the 45° roll to the upright position, the eyes did not completely rotate back to the initial torsional position but settled at a torsional offset position in the direction of the previous counterroll. In contrast to our study, however, the torsional offset position reported by Schworm et al. was not significantly different between the two eyes.

RT can be explained by assuming that the ocular motor system allows for some side-to-side play of torsion. Within this deadband, the actual torsion at a given moment is partly random (Straumann et al. 1996; Van Rijn and Collewijn 1994) and partly determined by the previous torsion that, for instance, is modulated by the otolith-ocular reflex. We conjecture that counterroll consists in a shift of the deadband, so that the momentary torsional position is no longer around the center of the deadband, but at the edge of the deadband, which lies opposite to the eye movement direction. In this way, torsion in upright position would depend on previous ocular counterroll. This hypothesis predicts that head roll to an ear-down position and back to upright again induces RT in the direction of the previous counterroll, which agrees with the result of Schworm et al. (2002). If roll continues further from the ear-down to complete a full 360° cycle, RT should be directed oppositely, which is in agreement with results of this study.

The fact that the second and third rotation cycle did not substantially change the amount of RT strongly supports our hypothesis of a mechanism with a defined side-to-side play, i.e., a fixed width of the deadband. It is important to realize that, within such a mechanism of hysteresis, there is no absolute torsional eye position. Rather, ocular torsion depends on the direction of rotation performed before reaching the momentary position. As a result, torsional eye position at a given turntable roll position is unambiguous only if the maximal amount of hysteresis has been reached. Whether this requires a full turntable rotation cycle or less is not yet clear. In any case, after the first full rotation cycle, torsional eye position is unequivocally determined by the turntable roll position.

Computer model with asymmetric backlash

Figure 9 depicts a computer model (written with Simulink, MathWorks, Natick, MA) of the otolith-ocular pathway focusing on the phenomenon of dissociated hysteresis of SOCR and RT. Note that this computer model solely represents the flow of graviceptive signals, but does not correspond to the exact anatomical otolith-ocular pathways. A straightforward way to model static hysteresis is with backlash. In a backlash block, a change in input causes an equal change in output, but because of the side-to-side play in the system, changes in the direction of the input initially have no effect on the output. Backlash is

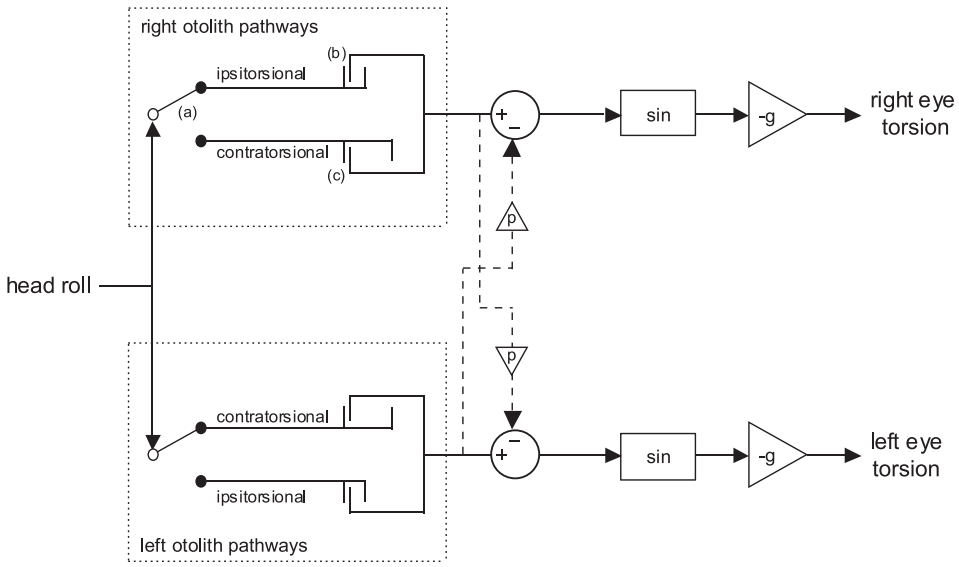

FIG. 9. Binocular asymmetric backlash model of static otolith-ocular reflex. Input is head roll about an earth-horizontal axis. Orientation of gravity vector in the head is encoded within the otolith pathways. Depending on whether the head is rolled in the ipsi- or contratorsional direction (*A*: switch) with respect to the otolith organ on either side, signal goes through a different backlash block. The deadband of backlash for head roll to the same side (*B*: ipsitorsional backlash) is smaller than for head roll to the other side (*C*: contratorsional backlash). Sine block implements sensorimotor transformation from otolith angular coordinates to torsional position of the eye, which saturates in ear-down side positions and is maximal at upright and upside-down. Note that the sine block is distal of otolith pathways (i.e., outside of dotted rectangle) and does not represent sensitivity of otolith sensors. Gain block ($-g$) takes into account that the eye torts in the opposite direction (negative sign) and that the static otolith-ocular reflex is not fully compensatory ($g < 1$). Model assumes predominant otolith projections to the motoneurons of the ipsilateral eye and therefore discounts contralateral projections (dashed pathways). Accordingly, corresponding gain block (p) was set to 0 for computer simulation.

not identical with hysteresis, but in mechanical systems, backlash is usually the main factor causing hysteresis.

By definition, backlash is symmetric, i.e., a side-to-side input signal results in symmetric hysteresis. To model asymmetric hysteresis, we therefore need a switch that changes the amount of side-to-side play of the backlash block, i.e., the width of the so-called deadband, according to the direction of head roll. Between the otolith input and the ocular motor output, the information of head roll direction is only available within the otolith pathways. After the roll movement of the head is transformed to a signal that contains eye torsion, it is no longer possible to determine the direction of head rotation. This is because the signal distal of the otolith pathways is ambiguous. For instance, an increasing CW ocular signal could indicate a movement from upright to right ear-down or a movement from upside-down to right ear-down. In both cases we would expect the same hysteresis, if the backlash would occur on the level of the ocular motor output. This, however, is not the case in our data. As a result, we had no choice than to implement asymmetric backlash at the level of the otolith pathways.

If the projections from the otoliths to the extraocular motoneuron pools on both sides were symmetric, asymmetries at the level of the otoliths would not result in dissociated hysteresis. Anatomical and electrophysiological data, however, suggest that the ipsilateral projections from the otolith organs to the extraocular motoneurons are more direct than the contralateral projections (Goto et al. 2003; Shimazu and Smith 1971; Suzuki et al. 1969; Uchino et al. 1996). In the model, we opted to set the gain of the contralateral pathways to zero, i.e., discard these projections.

Asymmetric backlash implies that repetitive roll movements of the head from side to side would lead to an increasing cyclovergence. Mechanisms that may prohibit this effect (e.g., resetting eye movements, backlash nonlinearities, or passive forces of the ocular plant) are not implemented in the model. Another experimental finding that is also not included in the computer model is the amplitude difference of the sine fit between CE and IE. The impact of this finding, however, is relatively small compared with the consequences of the dissociated hysteresis.

Figure 10 shows simulated binocular torsion during steady-state 360° rotations about the earth-horizontal naso-occipital axis of a subject. We assumed a position gain of 0.08 (eye torsion divided by head roll from upright). To better clarify the effect that evolves from less backlash during head roll in the ipsitorsional than in the contratorsional direction, the deadband was set to zero for ipsitorsional head roll and 20° for contratorsional head roll. Accordingly, during CW rotation, the torsional position of the right eye was in phase with the turntable, whereas the left eye lagged turntable position by 10° (Fig. 10*A*). Setting both torsional eye positions to zero at upright head position (definition of 0 torsion) shifted the curves such that the maximal extorsion of the left eye increased and the maximal cyclodivergence occurred in the upside-down position (Fig. 10*C*). Comparing torsional position of the right eye during turntable rotations in both directions shows asymmetric hysteresis with a position lag that only occurs during CCW rotation (Fig. 10*B*). Setting the torsional position to zero at upright head position revealed that both maximal intorsion and maximal extorsion are larger when they occur during the first hemicycle of the rotation (Fig. 10*D*), which is in accordance of our data. Note again that the asymmetric backlash model only predicts a different position lag between the eye that first intorts and the eye that first extorts, but not different amplitudes of sine fits between the two eyes.

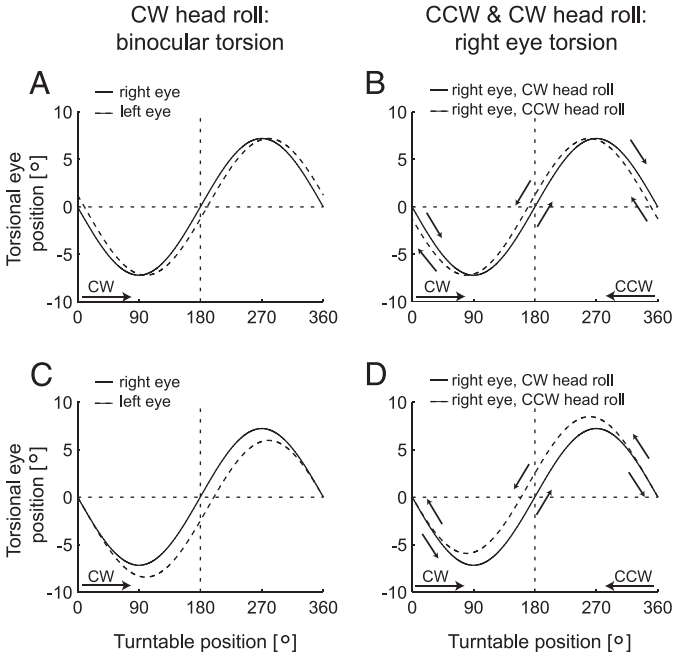

FIG. 10. Simulation of asymmetric backlash model. *A* and *C*: example of static hysteresis during CW rotation within both eyes. *B* and *D*: example of asymmetric static hysteresis of the right eye within CW and CCW head rotations. Deadband of ipsitorsional otolith backlash (leading to intorsion of ipsilateral eye): 0°. Deadband of contratorsional otolith backlash (leading to extorsion of ipsilateral eye): 20°. Position gain of static otolith-ocular reflex: $g = 0.08$. Gain of contralateral projection: $P = 0.00$. *Left*: binocular torsional eye position (right eye, solid line; left eye, dashed line) during CW roll. Left eye shows a position lag of 10°. *C*: binocular torsion is shifted to 0 in upright position (reference torsion). As a consequence, the left eye is extorted by 2.5° in the upside-down position leading to extorsion (right eye torsion is 0). *Right*: torsional positions of the right eye during head roll in both directions. No position lag during CW roll; 10° position lag during CCW roll. *D*: torsional position of the right eye is shifted to 0 in upright position. As a consequence, maximal intorsion and maximal extorsion is larger in the 1st than in the 2nd hemicycle.

In conclusion, we found dissociated torsional hysteresis during quasi-static binocular counterroll in healthy human subjects. A model that includes asymmetric backlash for each eye can explain this phenomenon. The model predicts that the hysteresis is introduced within the otolith pathways, not the eye plants, because the torsional direction-dependent position lag of the eyes is related to head roll position. Whether hysteresis occurs at the level of the sensors because of nonuniform movements of the otolithic membrane (Benser et al. 1993; Jaeger et al. 2002; Markham and Diamond 2001) or at the level of neurons that encode head position with respect to gravity remains to be explored.

We emphasize that dissociated torsional hysteresis does not imply an asymmetry between the otolith organs of the right and left labyrinths, because the characteristics of binocular hysteresis are mirrored between right ear-down and left ear-down counterroll. On the other hand, our results show possible asymmetries at the level of the otolith organs, which have been suggested by studies on ocular torsion during and after changes

of g, induced by parabolic flight or microgravity (Diamond and Markham 1998; Markham et al. 2000). Based on these results, it was hypothesized that the control of otolith-induced ocular torsion is independent between the two eyes (Markham and Diamond 2001; Markham et al. 2000). The existence of dissociated torsional hysteresis also suggests, at least partially, independent connections between the unilateral otolith sensors and the single eyes.

We can only speculate on how unilateral lesions of otolith organs may affect binocular SCOR. In analogy to studies in the recovery of the horizontal translational vestibulo-ocular reflex (Lempert et al. 1998), we predict that unilateral loss of otolith signals induces compensatory reorganization of the afferents from the intact otolith organ. This, in turn, could result in an upregulation of the pathways projecting to the contralateral side (Fig. 9, dashed pathway). As a consequence, the intact otolith organ solely would drive the extraocular motoneuron pools on both sides and thus hysteresis would no longer be dissociated. We are not yet able to confirm or reject this hypothesis. However, future studies on patients with unilateral vestibular deficits might provide further insights.

ACKNOWLEDGMENTS

We thank I. S. Curthoys for valuable comments on static ocular counter roll and S. Glasauer for helpful advice in modeling the static otolith-ocular reflex; three anonymous referees for helpful comments regarding the manuscript; S. Marti and K. P. Weber for help during the experiments; and E. Schafflützel, T. Schmückle, and A. Züger for technical assistance.

GRANTS

This study was supported by Swiss National Science Foundation Grant 3200B0-105434 and the Betty and David Koetser Foundation for Brain Research, Zurich, Switzerland.

REFERENCES

Angelaki DE and Hess BJ. Three-dimensional organization of otolith-ocular reflexes in rhesus monkeys. II. Inertial detection of angular velocity. *J Neurophysiol* 75: 2425–2440, 1996a.

Angelaki DE and Hess BJ. Three-dimensional organization of otolith-ocular reflexes in rhesus monkeys. I. Linear acceleration responses during off-vertical axis rotation. *J Neurophysiol* 75: 2405–2424, 1996b.

Averbuch-Heller L, Rottach KG, Zivotofsky AZ, Suarez JI, Pettee AD, Remler BF, and Leigh RJ. Torsional eye movements in patients with skew deviation and spasmodic torticollis: responses to static and dynamic head roll. *Neurology* 48: 506–514, 1997.

Benser ME, Issa NP, and Hudspeth AJ. Hair-bundle stiffness dominates the elastic reactance to otolithic-membrane shear. *Hear Res* 68: 243–252, 1993.

Bergamin O, Bizzarri S, and Straumann D. Ocular torsion during voluntary blinks in humans. *Invest Ophthalmol Vis Sci* 43: 3438–3443, 2002.

Bockisch CJ and Haslwanter T. Three-dimensional eye position during static roll and pitch in humans. *Vision Res* 41: 2127–2137, 2001.

Collewijn H, van der Steen J, Ferman L, and Jansen TC. Human ocular counterroll: assessment of static and dynamic properties from electromagnetic scleral coil recordings. *Exp Brain Res* 59: 185–196, 1985.

Crawford JD, Tweed DB, and Vilis T. Static ocular counterroll is implemented through the 3-D neural integrator. *J Neurophysiol* 90: 2777–2784, 2003.

Diamond SG and Markham CH. Ocular counterrolling as an indicator of vestibular otolith function. *Neurology* 33: 1460–1469, 1983.

Diamond SG and Markham CH. Changes in gravitational state cause changes in ocular torsion. *J Gravit Physiol* 5: 109–110, 1998.

Diamond SG, Markham CH, and Furuya N. Binocular counterrolling during sustained body tilt in normal humans and in a patient with unilateral vestibular nerve section. *Ann Otol Rhinol Laryngol* 91: 225–229, 1982.

Diamond SG, Markham CH, Simpson NE, and Curthoys IS. Binocular counterrolling in humans during dynamic rotation. *Acta Otolaryngol* 87: 490–498, 1979.

Glasauer S, Dieterich M, and Brandt T. Central positional nystagmus simulated by a mathematical ocular motor model of otolith-dependent modification of Listing's plane. *J Neurophysiol* 86: 1546–1554, 2001.

Goto F, Meng H, Bai R, Sato H, Imagawa M, Sasaki M, and Uchino Y. Eye movements evoked by the selective stimulation of the utricular nerve in cats. *Auris Nasus Larynx* 30: 341–348, 2003.

Haslwanter T, Straumann D, Hess BJ, and Henn V. Static roll and pitch in the monkey: shift and rotation of Listing's plane. *Vision Res* 32: 1341–1348, 1992.

Haustein W. Considerations on Listing's law and the primary position by means of a matrix description of eye position control. *Biol Cybern* 60: 411–420, 1989.

Hess BJ and Angelaki DE. Gravity modulates Listing's plane orientation during both pursuit and saccades. *J Neurophysiol* 90: 1340–1345, 2003.

Jaeger R, Takagi A, and Haslwanter T. Modeling the relation between head orientations and otolith responses in humans. *Hear Res* 173: 29–42, 2002.

Kingma H, Stegeman P, and Vogels R. Ocular torsion induced by static and dynamic visual stimulation and static whole body roll. *Eur Arch Otorhinolaryngol* 254(Suppl 1): S61–S63, 1997.

Krejcova H, Highstein S, and Cohen B. Labyrinthine and extra-labyrinthine effects on ocular counter-rolling. *Acta Otolaryngol* 72: 165–171, 1971.

Lempert T, Gianna C, Brookes G, Bronstein A, and Gresty M. Horizontal otolith-ocular responses in humans after unilateral vestibular deafferentation. *Exp Brain Res* 118: 533–540, 1998.

Markham CH and Diamond SG. Ocular counterrolling differs in dynamic and static stimulation. *Acta Otolaryngol Suppl* 545: 97–100, 2001.

Markham CH, Diamond SG, and Stoller DF. Parabolic flight reveals independent binocular control of otolith-induced eye torsion. *Arch Ital Biol* 138: 73–86, 2000.

Markham CH, Estes MS, and Blanks RH. Vestibular influences on ocular accommodation in cats. *Int J Equilib Res* 3: 102–115, 1973.

Nagel A. Ueber das Vorkommen von wahren Rollungen des Auges um die Gesichtslinie. *Arch Ophth* 14: 228–246, 1868.

Ott D, Seidman SH, and Leigh RJ. The stability of human eye orientation during visual fixation. *Neurosci Lett* 142: 183–186, 1992.

Palla A, Bockisch CJ, Bergamin O, and Straumann D. Residual torsion following ocular counterroll. *Ann NY Acad Sci* 1039: 81–87, 2005.

Pansell T, Tribukait A, Bolzani R, Schworm HD, and Ygge J. Drift in ocular counterrolling during static head tilt. *Ann NY Acad Sci* 1039: 554–557, 2005.

Pansell T, Ygge J, and Schworm HD. Conjugacy of torsional eye movements in response to a head tilt paradigm. *Invest Ophthalmol Vis Sci* 44: 2557–2564, 2003.

Schworm HD, Ygge J, Pansell T, and Lennerstrand G. Assessment of ocular counterroll during head tilt using binocular video oculography. *Invest Ophthalmol Vis Sci* 43: 662–667, 2002.

Seidman SH, Leigh RJ, Tomsak RL, Grant MP, and Dell'Osso LF. Dynamic properties of the human vestibulo-ocular reflex during head rotations in roll. *Vision Res* 35: 679–689, 1995.

Shimazu H and Precht W. Tonic and kinetic responses of cat's vestibular neurons to horizontal angular acceleration. *J Neurophysiol* 28: 991–1013, 1965.

Shimazu H and Smith CM. Cerebellar and labyrinthine influences on single vestibular neurons identified by natural stimuli. *J Neurophysiol* 34: 493–508, 1971.

Straumann D, Zee DS, Solomon D, and Kramer PD. Validity of Listing's law during fixations, saccades, smooth pursuit eye movements, and blinks. *Exp Brain Res* 112: 135–146, 1996.

Suzuki JI, Tokumasu K, and Goto K. Eye movements from single utricular nerve stimulation in the cat. *Acta Otolaryngol* 68: 350–362, 1969.

Uchino Y, Sasaki M, Sato H, Imagawa M, Suwa H, and Isu N. Utriculoocular reflex arc of the cat. *J Neurophysiol* 76: 1896–1903, 1996.

Van Rijn LJ and Collewijn H. Eye torsion associated with disparity-induced vertical vergence in humans. *Vision Res* 34: 2307–2316, 1994.

Van Rijn LJ, van der Steen J, and Collewijn H. Instability of ocular torsion during fixation: cyclovergence is more stable than cycloversion. *Vision Res* 34: 1077–1087, 1994.

Yashiro T, Ishii M, Igarashi M, Kobayashi T, Moriyama H, and Sekiguchi C. Effects of 10 min tilt and visual directional information on ocular counterrolling. *ORL J Otorhinolaryngol Relat Spec* 58: 301–303, 1996.